than for prediction of crown deflection. The comparison between results obtained through use of the graphs and those from the specific finite-element analysis was encouraging. For similar values of E_s = 30 MPa the difference in deflection results was 5 percent, whereas the difference in thrust was negligible. This would suggest that the graphs based on the idealized system geometry can be applied to cases where details are somewhat different from the ideal system. Agreement is also demonstrated between predictions of springline thrust and field measurements. Two of the three pertinent strain-gauge results show agreement with predictions within a few percentage points. (It is notable that, for this case, a computation based on the ring compression theory gives a springline thrust that is about 25 percent too low.)

Crown deflection is not predicted with the same level of reliability. Total deflection associated with fill load up to 1.9 m of fill was predicted approximately 70 percent higher than the average measured deflection. (Deflection due to the final 0.2 m of fill could not be separated from that due to heavy-truck loading, according to a paper in this Record by Kay and Flint.) Calculations were based on soil modulus of 30 MPa determined from laboratory triaxial test measurements on the reconstituted granular soil. As demonstrated in Figure 22, a value of E_s = 60 MPa would have given a better estimate. However, it is notable that during the initial fill period over the crown, the measured deflection was small and, in the later stages, the slopes of the as-measured graphs are similar to those of the graphs based on predictions. This performance suggests an explanation in terms of construction procedure. The initial layers of fill placed over the crown do not receive the full compactive effort but are compacted by hand-held equipment. The effect of reduced compaction is considerably greater compressibility of the fill in this zone than the general compressibility, and as the general soil system moves downward with compression of the sidefills, the crown area of the arch, instead of moving downward in a similar fashion, penetrates the zone of more compressible soils. It is likely that improvement to prediction of crown deflection would result if zero deflection were assumed to occur to the level where mechanical compaction has begun. However, further observation of field installations is necessary to justify such an approach.

The effect of the heavy-vehicle live loading on crown deflection is considerable. This is the subject of the paper in this Record by Kay and Flint.

SUMMARY AND CONCLUSION

Graphs have been presented that enable prediction of crown deflection and springline thrust for systems of soil and corrugated-metal arches subject to loads from compacted fills placed above the crown level. Stepwise application of the graphs can minimize errors associated with nonlinear effects for conditions within the working-load range. Comparisons made between predictions based on the graphs and results of field measurements show reasonable agreement.

No recommendations are made concerning criteria for safe design in terms of these aspects of response. Insufficient research on the collapse of such structures has been completed to date to enable suggestions along these lines. Both large-scale testing and analytical work are in progress at the University of Adelaide through which it is hoped to contribute to some preliminary guidelines to a more complete design procedure in the future.

REFERENCES

1. E.T. Selig, J.F. Abel, F.H. Fulhawy, and W.E. Falby. Review of the Design and Construction of Long-Span, Corrugated-Metal, Buried Conduits. FHWA, Interim Rept. FHWA-RD-77-131, 1977.
2. J.G. Abel, G.A. Nasir, and R. Mark. Stresses and Deflections in Soil Structure Systems Formed by Long-Span Flexible Pipe. Department of Civil Engineering, Princeton Univ., Princeton, NJ, Res. Rept. 77-SM-13, 1977.
3. J.M. Duncan. Finite-Element Analysis of Buried Flexible Metal Culvert Structures. Laurits Bjerrum Memorial Volume, March 1975.
4. C.S. Chang, J.M. Espinoza, and E.T. Selig. Computer Analysis of Newtown Creek Culvert. Journal of the Geotechnical Engineering Division of ASCE, Vol. 106, No. GT5, 1980, p. 531.
5. M.G. Spangler. Culverts and Conduits. In Foundation Engineering (G.A. Leonards, ed.), McGraw-Hill, New York, 1962.
6. J.N. Kay and R.C.L. Flint. Design Charts for Large-Span Metal Arch Culverts. Department of Civil Engineering, Adelaide Univ., Australian Road Res. Board, Interim Rept., 1978.
7. M.G. Katona, D.F. Meinhart, T. Orillac, and C.H. Lee. Structural Evaluation of New Concepts for Long-Span Culverts and Culvert Installations. FHWA, Interim Rept. FHWA-RD-79-115, 1979.
8. J.N. Kay, D.L. Avalle, R.C.L. Flint, and C.F.R. Fitzhardinge. Instrumentation of a Corrugated Steel-Soil Arch Overpass at Leigh Creek, South Australia. Proc., 10th Conference of Australian Road Res. Board, Vol. 10, No. 3, 1980, pp. 57-70.

Publication of this paper sponsored by Committee on Subsurface Soil-Structure Interaction.

Analysis of Live-Load Effects in Soil-Steel Structures

GEORGE ABDEL-SAYED AND BAIDAR BAKHT

This paper is based on an analytical study undertaken to complement a previously reported experimental study on live-load effects in the metallic shell of a soil-steel structure. An account of load dispersion above the conduit cannot be made by neglecting the presence of the conduit. The plane-strain approach of analyzing a soil-steel structure is found to be a defensible one even for concentrated loads. It is found that the manner of load dispersion in the longitudinal direction of the conduit is distinctly different from that in the transverse direction. This observation confirms previously reported experimental results. A simplified method, which at best is a crude approximation, can only pick up the maximum thrust values in the conduit wall and is dependent on the con-

figuration of the design vehicle. The Ontario Highway Bridge Design Code method is found to be applicable only when there is a pair of closely spaced axles on the embankment. When the governing load is made up of a single axle, another simplified method is proposed.

Underground conduits of relatively large spans [up to 55 ft (16.75 m)] are being built in increasing number for use as culverts, bridges, and tunnels. It has been usual in the past to idealize these structures for analysis by plane-strain transverse slices of the metallic shell and the surrounding soil envelope. The inherent assumption in this kind of idealization is that load effects due to both dead and live loads do not vary along the conduit. This assumption may be axiomatic for dead loads but needs a rational scrutiny for live loads, especially because of the trend for larger spans and shallow depths of cover, which together tend to make live-load effects a fairly large proportion of the total load effects in the metallic shell.

This paper is based on the results of an analytical study of the distribution of concentrated live loads in soil-steel structures. The study, which was undertaken at the University of Windsor in cooperation with the Ministry of Transportation and Communications of Ontario, complements the experimental work reported elsewhere (1). In this study the dispersion of concentrated loads through the soil is examined by taking into account the different geometric conditions along the conduit axis and in the transverse direction. A simple analysis procedure, similar to those currently employed, is developed to realistically assess live-load effects in the metallic shell.

LIVE-LOAD DISPERSION IN SOIL

Several solutions are available in published literature to calculate the stress distribution (or load dispersion) in soil due to concentrated point or line loads. Some of the various assumed soil characteristics and boundary conditions relevant to the different solutions can be summarized as follows (2,3):

1. Homogeneous isotropic half-space: The soil is assumed to be of semiinfinite extent, and its modulus of elasticity (E_s) is considered to be constant.

2. Homogeneous isotropic finite layer: The soil is assumed to have finite depth and to be supported by a rigid subsurface.

3. Nonhomogeneous half-space: The soil is again assumed to be of semiinfinite extent, but its modulus of elasticity varies with depth according to the following relationship:

$$E_s = E_0 \cdot (z/z_0)^{\lambda} \quad (1)$$

where E_0 is the modulus of elasticity at a depth $z = z_0$, z is the depth of soil under consideration, and λ is a constant ≥ 0.

4. Cross-anisotropic half-space: The soil is assumed to be of infinite extent and its degree of anisotropy is expressed by the ratio of the moduli of elasticity in the horizontal and vertical directions (E_h/E_v), the ratio of the shear modulus to the vertical modulus of elasticity (G/E_v), and the Poisson's ratios μ_h and μ_{hv}.

Solutions based on the above assumed conditions give widely differing patterns of stress distribution in the soil, as shown in Figure 1, which shows the variation of $I_{\sigma z}$ corresponding to a point load (P). Vertical stress (σ_v) is given by the following relationship:

$$\sigma_v = I_{\sigma z} P/z^2 \quad (2)$$

where z is the depth at which the stress is investigated. Figure 1 is instructive in studying the various factors that have a significant influence on load dispersion in soil.

A comparison of the $I_{\sigma z}$ values corresponding to the assumptions of "isotropic half-space" and "isotropic finite layer" (in which the stresses are calculated at the level of the supporting surface) shows that the peak vertical stress in the former case is considerably less than that in the latter case; thus the significance of the relative stiffness of the underlying layer on load dispersion is emphasized. It can be readily concluded that the insertion of a conduit in a half-space would have the effect of changing the soil stiffness, and therefore the load dispersion above the conduit cannot be justifiably obtained by neglecting the presence of the conduit, i.e., by assuming the soil to be homogeneous.

Figure 1. Pressure distribution under concentrated load.

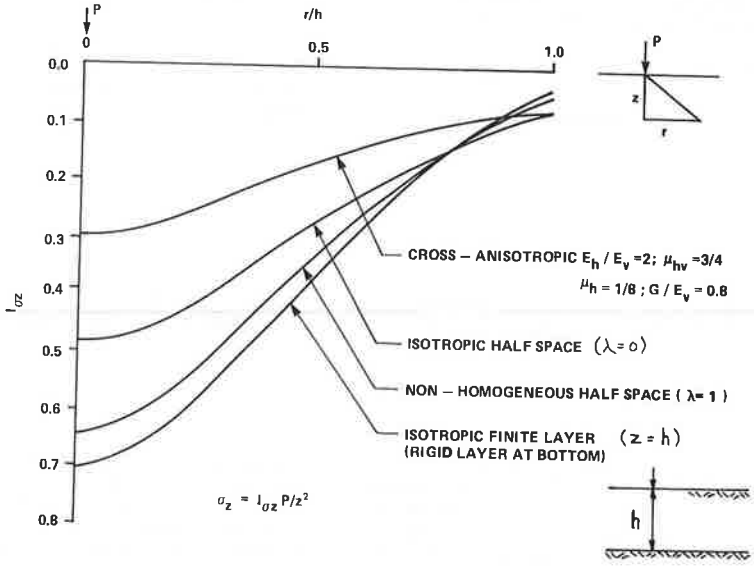

Figure 2. Load dispersion through soil.

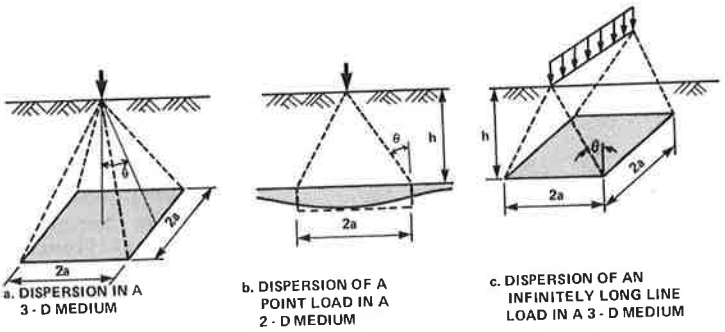

Table 1. Comparison of different approaches for obtaining equivalent areas.

Soil Idealization and Boundary Condition	$\alpha = h/a$			$\theta°$		
	Approach 1	Approach 2	Difference (%)	Approach 1	Approach 2	Difference (%)
Isotropic half-space	1.37	1.27	7.4	35.9	38.1	5.6
Isotropic finite layer	1.66	1.87	1.6	31.0	31.4	1.3
Nonhomogeneous half-space						
$\lambda = 1$	1.60	1.50	6.2	32.0	33.6	4.8
$\lambda = 2$	1.79	1.69	5.1	29.3	30.5	3.9
$\lambda = 3$	1.96	1.87	4.6	27.0	28.1	4.1

Note: Approach 1 corresponds to the three-dimensional analysis and Approach 2 to the two-plane method.

Figure 3. Load dispersion above conduit.

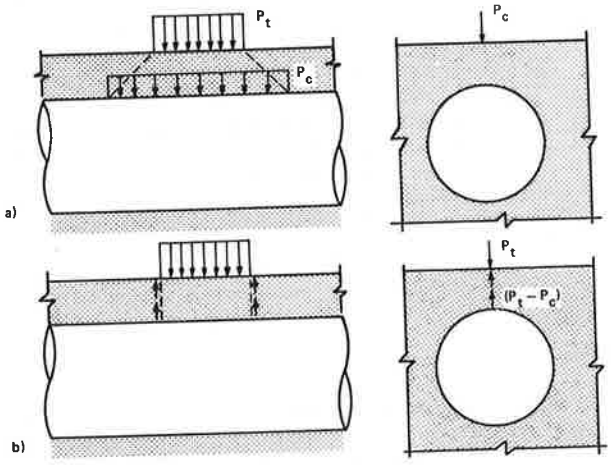

From Figure 1 it can also be observed that the vertical stress concentration in the homogeneous soil is lower than that in the nonhomogeneous soil in which the modulus of elasticity increases linearly with depth. The decrease in the stress concentration is also caused by the increase of the shear modulus of the soil.

LOAD DISPERSION IN SOIL BY PLANE STRAIN

When an elastic half-space is subjected to a concentrated load P at the boundary, the vertical stress under the load at a plane parallel to the boundary can, for the sake of convenience, be assumed to be uniformly distributed over an effective 2ax2a area. This equivalent area is such that its product with the peak vertical stress is equal to the load P. Let the depth of the level at which the equivalent area is sought be denoted by h and the angle of dispersion to the vertical by θ (Figure 2).

The equivalent area under a point load can be obtained by considering dispersion in the three-dimensional medium, as shown in Figure 2a. Alternatively, the load can first be dispersed in only one plane (Figure 2b) and then the resulting maximum load per unit width acting at the depth h is reapplied as a line load to the boundary and dispersed in the perpendicular plane (Figure 2c). The latter approach has often been applied for establishing equivalent live loads on the plane-strain slice of the soil-steel structures, and the former approach has often been the basis of simplified methods of analyzing live-load effects in the metallic shell (1). The following exercise was undertaken to establish the degree of error involved if the latter approach were adopted.

Equivalent distributed areas corresponding to a single concentrated load were obtained for various idealized soil media and different boundary conditions according to the two above-mentioned procedures. Values of $\alpha = h/a$ and θ obtained by the two procedures are compared in Table 1 for different cases. It can be seen that the procedure of distributing the load first in one plane and then in another produces results that are not significantly different from those obtained by the corresponding three-dimensional analysis; thus the use of the two-plane analysis approach in the analysis of soil-steel structures is justified.

As observed by Bakht (1), the dispersion of a concentrated load in the longitudinal direction of a conduit is significantly different from that in the transverse direction. An account of this different dispersion pattern can be made by first distributing the load in the longitudinal direction and then applying the dispersed load on the transverse slice as shown in Figure 3a; alternatively, as shown in Figure 3b, the full concentrated load can be applied directly at the top of the soil along with subsurface negative upward forces accounting for the load dispersed to the adjacent slices in the longitudinal direction. The two methods were used to analyze two soil-steel structures described by Bakht (1) by the plane-strain finite-element method. As shown in Table 2, the difference between the thrust and moment predictions by the two methods does not amount to more than 5 percent. This comparison

further justifies the use of the two plane-strain approaches to live-load analysis of soil-steel structures.

LOAD DISPERSION ALONG CONDUIT

It is assumed that the problem of load dispersion along the conduit can be independently solved by isolating a longitudinal unit-width slice of soil above the crown. As shown in Figure 4, the support provided by the metallic shell is simulated by uniformly spaced linear springs. The spring stiffness K, which represents the ratio of pressure to deflection at the crown, was found by analysis of soil-steel structures to be of the order of 60 psi/in. It was decided to scan values of K between 30 and 300 psi/in for the study discussed below.

The plane-strain finite-element method (4) was used to analyze the longitudinal slice for the two load cases of direct wheel pressure as shown in Figure 4. The analyses are based on a nonlinear soil model developed by Wong and Duncan (5). Three types of soil are considered for which the properties are given in Figure 5a. Figure 5a also shows the distribution of σ_v corresponding to load case 1 (Figure 4) for the three types of soil. As expected, the peak value of σ_v increases with the decrease of soil stiffness. Also, as shown in Figure 5b, the peak value of σ_v increases with the increase of the spring stiffness.

The load dispersion in the longitudinal direction can be approximately represented by an equivalent length that, as shown in Figure 6, has a projection of length (a) beyond the extremity of the surface load. For the two load cases mentioned earlier and considering soil type B (Figure 5a), the relationship between $\alpha = h/a$ and K is plotted in Figure 6. It can be seen that the depth of cover has relatively little influence on this relationship. It is noted that the current simplified methods of the American Association of State Highway and Transportation Officials (AASHTO) (6) and the Ontario Highway Bridge Design Code (OHBDC) (7) do not account for the stiffness of the metallic shell. For the former, the value of α is 1.14 and for the latter, 2.0. These two values of α are compared in Figure 6 with those obtained by the finite-element analysis. It can be observed that both methods give results that are distinctly different from those of the finite-element analysis. However, for values of K that are usually encountered in practice, the OHBDC method is in error on the safe side. It is noted that the effect of error in estimation of α is reduced in practice because of the finite length of the concentrated load.

The relationship between α and K can be represented in hyperbolic form:

$$\alpha = K/(c + bK) \tag{3}$$

where c and b are constants depending on the properties of soil. Equation 3 can be rewritten in the form of a linear relationship between K and (K/α):

$$(K/\alpha) = C + bK \tag{4}$$

This linear relationship is confirmed in Figure 7, which shows that although the relationship between α and (K/α) is independent of the depth of cover, it still depends on the configuration of applied loading. For given soil properties and load cases, it is possible to determine values of constants b and c from graphs such as that shown in Figure 7. From values obtained of b and c, charts could be prepared to readily provide the values of constants and thence the value of α from Equation 3. However, for everyday designs the process would still be too tedious and not worth the effort, and it is recommended that a value of α equal to 2.0 be used for all practical purposes.

Table 2. Comparison between analytical results by using methods a and b, Figure 3, for live load.

Beam Element No.	Thrust (lbf/in)				Moment (lbf·in/in)	
	White Ash Creek Structure[a]		Adelaide Creek Structure[a]		Adelaide Creek Structure[a]	
	Loading a	Loading b	Loading a	Loading b	Loading a	Loading b
1	-16.6	-11.5	10.8	14.5	5.9	6.0
3	-19.0	-16.2	-19.9	-19.0	1.0	1.3
5	-41.2	-41.1	-59.0	-59.8	-26.0	-26.6
7	-87.5	-89.7	-77.5	-79.0	6.5	5.2
9	-156.7	-161.1	-84.8	-86.6	1.8	0.6
11	-239.3	-246.0	-235.3	-242.3	-60.3	-65.5
13	-239.3	-246.0	-235.2	-242.2	4.9	3.9
15	-298.9	-307.8	-321.6	-332.1	69.4	72.9
17	-299.0	-307.8	-321.7	-332.2	84.1	87.1
19	-337.2	-350.1	-385.9	-400.6	97.3	100.0
21	-337.2	-350.2	-385.9	-400.6	90.0	93.6
23	-289.7	-307.0	-399.9	-420.5	82.4	86.9
25	-289.6	-307.0	-399.8	-420.3	41.6	45.0
27	-150.7	-167.1	-201.2	-218.6	4.6	7.1
29	-149.7	-166.1	-200.5	-217.8	-67.2	-70.4

[a]For details of structure, see report by Bakht (1).

LOAD DISPERSION IN SPAN DIRECTION

After the approximate equivalent live load on the plane-strain slice of a soil-steel structure had been established, the slice was analyzed by a special-purpose plane-strain finite-element program incorporating high-order nonlinear elements to model the soil, beam elements to simulate the metallic shell, and nonlinear interface elements to represent the bond between the soil and the metallic shell (4). Effects of the construction procedure were taken into account by an iterative process in which the equivalent of compaction loads was applied at various backfill levels. Structures tested by Bakht

Figure 4. Idealization for load dispersion along conduit axis.

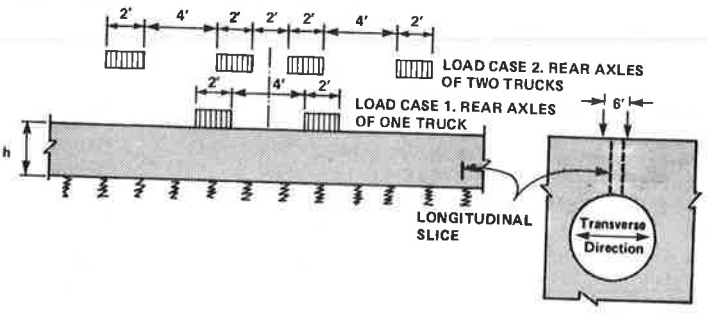

Figure 5. Effect of soil type and spring constants on load dispersion through soil along conduit.

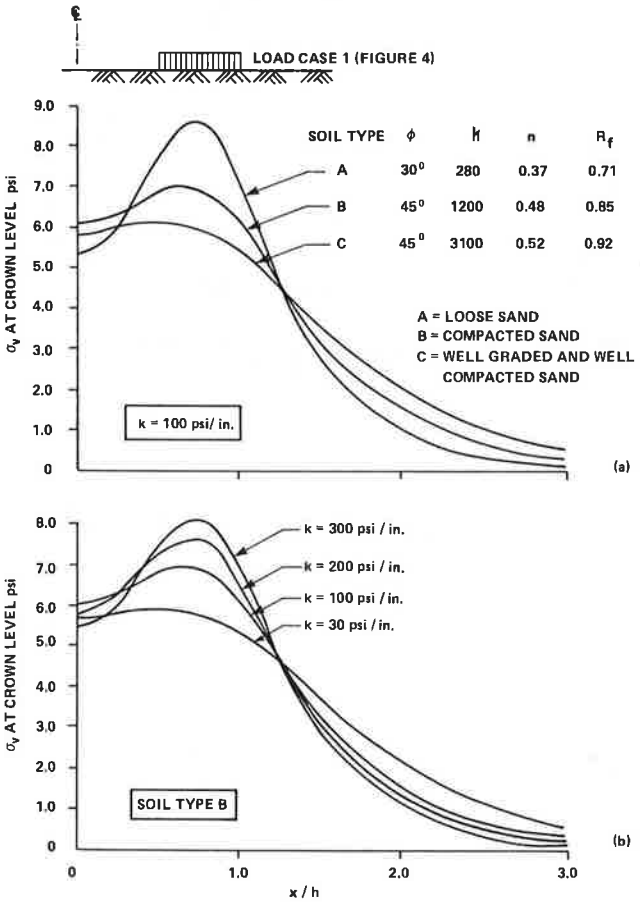

Figure 6. Comparison of various methods accounting for load dispersion along conduit.

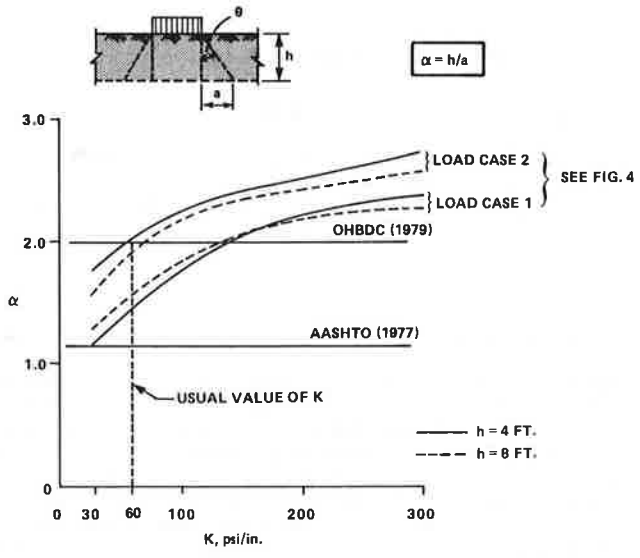

(1) were analyzed for live-load effects by the above procedure. The correlation between the analytically obtained and observed values of conduit wall thrust and moments, although not quite perfect, was reasonably good. Comparisons between the analytical and

Figure 7. Relationship between K and (K/α).

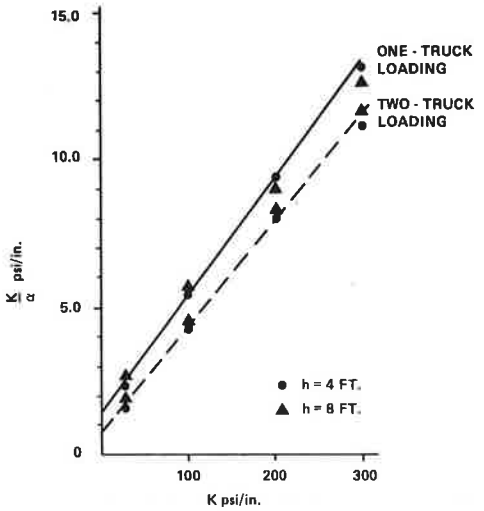

observed values of the conduit wall thrust are shown in Figure 8 for two load cases on one structure. It can be seen that with the analytical approach it is possible to reasonably predict the peak values of thrust and also the pattern of thrust around the conduit.

From the tests and analyses it was observed that the peak value of thrust due to live load takes place at the shoulders and that this value is maximum when the loads are placed symmetrically to the crown. The study described later was therefore limited to only symmetrical load cases.

Analytical results showed that the vertical soil pressures at crown level due to concentrated loads at the embankment level were fairly widely distributed across the span, as shown in Figure 9. This observation confirms the experimental findings of Bakht (1), which indicated that a concentrated load disperses over a greater length in the transverse direction of the conduit than it does along the conduit.

An insight into the composite action between the soil and the metallic shell can be obtained by studying the conduit wall thrust and soil stresses as obtained from the finite-element analysis and shown in Figure 10. It can be seen that with the exception of soil above the conduit, the maximum soil stresses are more or less tangential to the conduit wall. The variation in conduit wall thrust can be attributed to the bending action of the composite arch made out of the metallic shell and the surrounding soil envelope.

SIMPLIFIED METHOD

Although the finite-element method has been shown above to be capable of realistically predicting live-load thrust in the conduit wall, its use for everyday design is not recommended because of its complexity. A more appropriate role for the finite-element method would be in studying the behavior of the structure and in establishing the validity of existing simplified methods, such as those described by Bakht (1).

The nonlinear finite-element method, discussed above and described by Hafez (4), was used to validate the AASHTO (6) and the revised OHBDC methods described by Bakht (1). According to the AASHTO method, conduit wall thrust (T_L) due to live load is given by the following:

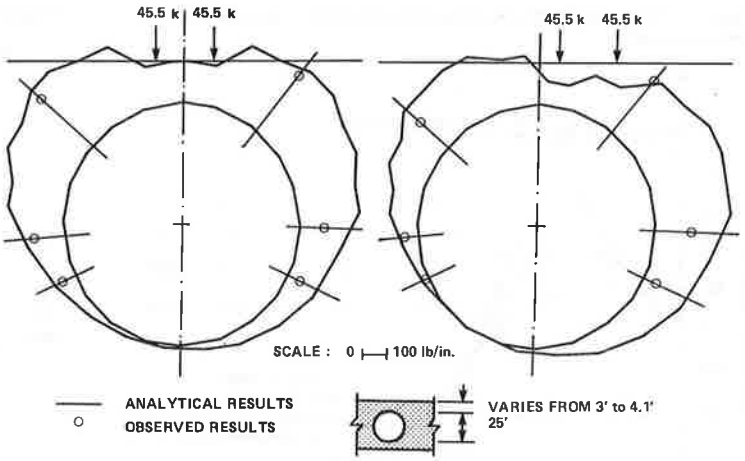

Figure 8. Comparison of observed and analytical thrust in conduit wall of soil-steel structure.

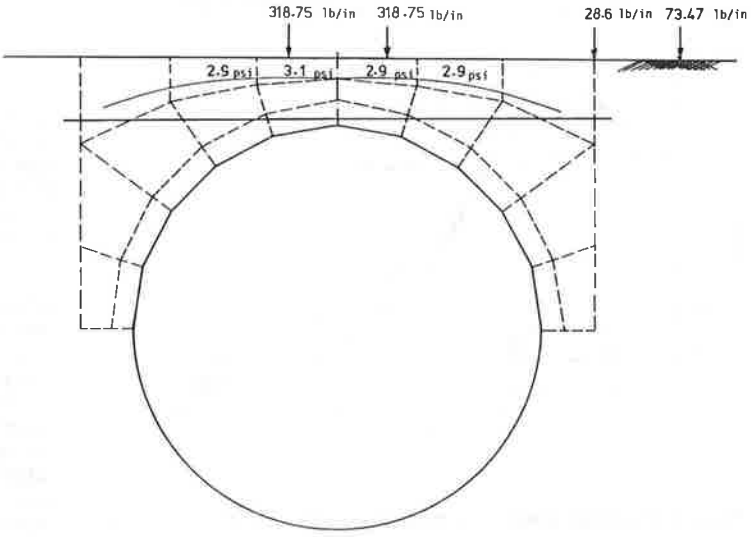

Figure 9. Vertical pressure in soil at crown level due to live loading.

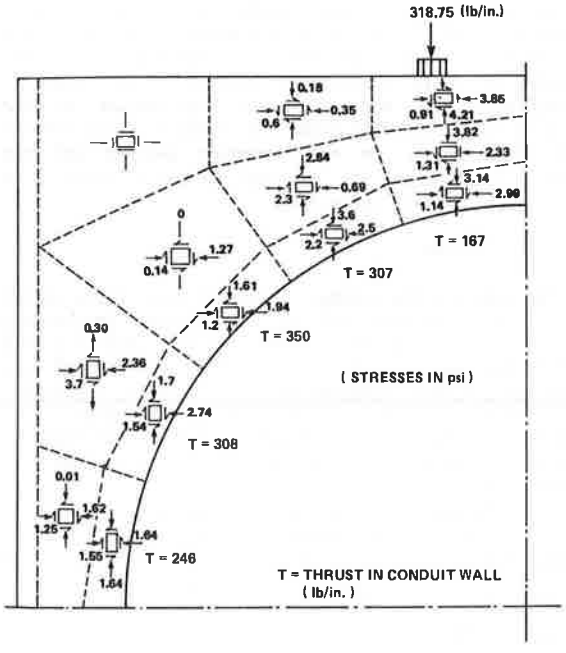

Figure 10. Analytical soil stresses around conduit due to live loading.

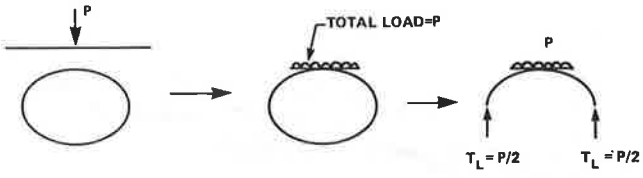

Figure 11. Thrust from equivalent load on transverse slice.

$$T_L = 0.5\sigma_L (1 + I) D_h \quad (5)$$

where D_h is the conduit span, I is the impact factor, and σ_L is the equivalent distributed load at crown level, obtained by assuming that the dispersed load is uniformly distributed over a square the sides of which are equal to 1.75h.

According to the revised OHBDC method, σ_L is obtained by assuming that the live load disperses at a 1:1 slope in the direction of the conduit span and at an angle of two vertical to one horizontal along the conduit length. The live-load thrust is then obtained by multiplying σ_L with the smaller of half the conduit span and half the length of the distributed load along the span (Figure 11).

A comparison of the AASHTO and OHBDC live-load thrust values with those obtained by the finite-ele-

Table 3. Comparison of maximum thrust values given by various methods.

Conduit Shape	Loading	Assumed Loading on Plane-Strain Slice (lbf/in)	h (in)	D_h (in)	D_h/D_v	Maximum Thrust (lbf/in)			
						Finite Element	OHBDC	AASHTO	Proposed for AASHTO
Circular	↓	306	48	300	1.0	192	153	390	227
	↓	302	96	300	1.0	127	153	176	116
	↓ ↓ ←72 in→	2 x 153	48	300	1.0	168	153	210	173
	↓ ↓ 48 in ←→	2 x 437	96	300	1.0	392	437	606	297
	↓ ↓ ←72 in→	2 x 153	48	150	1.0	100	128	147	87
Vertical ellipse	↓	306	46	300	0.625	180	153	250	227
	↓ ↓ ←72 in→	2 x 153	48	300	0.625	142	153	135	168
	↓ ↓ ←72 in→	2 x 153	48	150	0.625	99	86	70	84
Horizontal ellipse	↓	306	48	300	1.6	224	153	530	227
	↓ ↓ 48 in ←→	2 x 163	96	300	1.6	163	163	310	111
	↓ ↓ ←72 in→	2 x 153	48	300	1.6	168	153	285	168
	↓ ↓ ←72 in→	2 x 153	48	150	1.6	99	153	143	84

ment method (by using the properties of soil C, Figure 5a) for various cases is given in Table 3. It can be seen that the AASHTO method grossly overestimates live-load thrust in most cases. The revised OHBDC method gives closer answers to the finite-element method; however, it tends to underestimate the thrust corresponding to the single-axle loading case. It is noted that the combined weight of the dual axles (consisting of axles 4 ft apart) of the OHBDC design vehicle is 40 percent higher than the weight of the heaviest single axle. In this case the governing loading for conduit wall design is always made up of the dual axles. Therefore, it can be concluded that the revised OHBDC method gives adequate results corresponding to the OHBDC vehicle.

For governing single axles, as is the case for AASHTO design loadings, it is proposed to calculate the live-load conduit wall thrust according to Equation 5 after considering the axle load to be dispersed in the span direction at one vertical to two horizontal. Results obtained from this proposed simplified method are also given in Table 3. It can be seen that for single-axle loads, this approach yields safe and yet fairly accurate values of maximum live-load thrust.

OBSERVATIONS

A scrutiny of live-load thrust values obtained by the finite-element method will readily show that some of the basic assumptions on which the simplified methods are based are not entirely correct. For example, in the OHBDC method it is assumed that the equivalent distributed load within the span is entirely supported by the conduit wall thrust as shown in Figure 11. If this assumption were correct, then for loads that have an equivalent distributed load well within this span, the thrust would be in the same proportions as the loads. This is not true, as can be seen by comparing finite-element thrusts in rows 1 and 3 of Table 3, which show values of 192 and 168 lbf/in for the same total applied loads. It is observed that a simplified method at best is a crude approximation for solving an extremely complex problem.

CONCLUSIONS

It has been shown that live-load effects in the metallic shell of a soil-steel structure can be realistically calculated by first considering load distribution in the longitudinal direction of the conduit and then analyzing a transverse plane-strain slice of the structure. A concentrated load disperses more rapidly in the transverse direction than in the longitudinal direction.

In spite of the complexity of the problem and the inability of simplified methods to account for all the factors responsible for load dispersion, the use of a simplified method for everyday design-office use is attractive. The revised OHBDC method was found to be adequate only when the governing loading consists of a pair of closely spaced axles, as is the case for the OHBDC design loading. A new method is proposed for isolated single axles such as those of the AASHTO design vehicles.

REFERENCES

1. B. Bakht. Soil-Steel Structure Response to Live Loads. Journal of the Geotechnical Division of ASCE, June 1981, pp. 779-798.
2. D.M. Burmister. General Theory of Stresses and Displacements in Layered Soil Systems. Journal of Applied Physics, Vol. 16, No. 2, 1945, pp. 89-96; No. 3, pp. 126-127; No. 5, pp. 296-302.
3. H.G. Poulos and E.H. Davis. Elastic Solutions for Soil and Rock Mechanics. Wiley, New York, 1974.
4. H. Hafez. Soil-Steel Structures Under Shallow Covers. Univ. of Windsor, Windsor, Ontario, Ph.D. thesis, 1981.
5. K.S. Wong and J.M. Duncan. Hyperbolic Stress-Strain Parameters for Nonlinear Finite Element Analyses of Stresses and Movements in Earth Masses. Univ. of California, Berkeley, Geotechnical Engineering Rept. TE 74-3, 1974.
6. Standard Specifications for Highway Bridges. AASHTO, Washington, DC, 1974.
7. Ontario Highway Bridge Design Code. Ministry of Transportation and Communications, Downsview, Ontario, 1979.

Publication of this paper sponsored by Committee on Subsurface Soil-Structure Interaction.